Defect formation in Si(111)7×7 surfaces due to 200 eV Ar^+ ion bombardment

S. K. Ghose,[1,*] I. K. Robinson,[1] and R. S. Averback[2]
[1]*Department of Physics, University of Illinois, Urbana, Illinois 61801, USA*
[2]*Department of Material Science and Engineering, University of Illinois, Urbana, Illinois 61801, USA*
(Received 24 June 2003; published 28 October 2003)

Surface x-ray diffraction measurements have been made to study defect formation at the atomic level in the near surface region of Si(111)7×7 surface during low energy (200 eV) Ar^+ ion bombardment. We have observed the two characteristics of the defects: missing atoms at different layers in the surface region as well as outward strain. We provide calculations that demonstrate how crystal truncation rod (CTR) measurements are sensitive to these modifications in the surface regions. We find that the measurement is sensitive to lattice strain and site occupancy of individual atomic layers near to the surface. We have thus determined occupancy profiles that represent the density of missing atoms with depth after irradiation. Both the strain and the atom deficit are found to increase with dose while the two distributions extend to about the same depth. These results are consistent with simulations of the ion-solid interaction mechanism using SRIM2000 with appropriate choice of surface and bulk displacement energies.

DOI: 10.1103/PhysRevB.68.165342 PACS number(s): 68.47.Fg, 61.72.Dd, 61.80.Jh, 81.65.Cf

I. INTRODUCTION

The interaction of low-energy (less than a few hundred eV) ions with semiconductor surfaces has been intensively studied because ion irradiation is widely used in material processing,[1] for example, ion sputtering[2–5] and beam assisted epitaxial growth[6–9]. Nevertheless the details of defects formation at these low energies is only poorly known, owing to the difficulties introduced by surface relaxation and other effects of surfaces. It has been reported[8] that ion assisted reaction caused by physical bombardment is possible above $E=15$ eV, called the "displacement threshold energy" and other damage caused below ~15 eV is mostly attributed to chemical reactions. Physical phenomena at surfaces depend on the surface displacement energy, which will be in general be different from the bulk. A typical value of surface displacement energy for Si might be ~5 eV, crossing over to the bulk value of 15 eV beyond a certain depth. We are interested in the present work on investigating defect production in this crossover between the surface and the subsurface regions.

We have chosen Si(111)7×7 reconstructed surface as a model system, because it is a well-studied surface with three distinct layers available to chemical or physical interactions. Previous work has involved mainly STM measurements made on a Si(111)7×7 surface to study the surface defects formed by rare-gas ions in the energy ranges between 200 eV to 3 keV.[10–14] They observed that low energy (<500 eV) Ar or Xe ion bombardment on Si(111)7×7 surface leads to clearly identified surface defects. These surface defects are populated by adatom vacancy regions, where adatoms have been removed by ion impact. The possibility of sputtering from second and third layer of atoms has been demonstrated by molecular-dynamics simulation[15] and experiment[16] on different semiconductor surfaces. For our range of energy, the ion range and energy distribution is expected to extend beyond ~6 Å,[17] so there is a possibility of displacement of atoms below the surface layers. Since STM measurements are limited to the top surface layer, any defects below the first layer are unknown from these studies.

Surface x-ray diffraction, particularly crystal truncation rod (CTR) measurements have been a very successful technique to probe multiple layers near a surface and obtain three-dimensional (3D) information.[18] In this work, we have used surface x-ray diffraction CTR measurements to reveal the surface and sub-surface structure before and after low-energy (200 eV at 20° angle) Ar^+ interaction with the Si(111)7×7 reconstructed surface. In this paper, we first illustrate the ability of CTR measurements to obtain the Si(111)7×7 reconstructed surface as well as the bulk structure. We then show from calculations, how the measurement is sensitive to lattice strain and site occupancy of atoms within a few layers of the surface. We then explain our experimental procedure and describe the results based on the least squares fitting with the ROD (Ref. 19) analysis program. In the discussion the experimental results are compared with Monte Carlo simulation of damage in the surface and subsurface regions.

II. MODELS OF SURFACE DAMAGE

The lattice sum of a 3D crystal produces a reciprocal lattice of δ functions. The scattered intensity is then restricted by the Laue condition in all three directions.[20] For a crystal with finite size, this condition is relaxed and the scattered intensity extends over a volume in reciprocal space inversely proportional to the size of the crystal. If the crystal is cleaved in one direction to produce a flat surface, then scattering will no longer be isotropic and streaks of scattering appear in the direction parallel to the surface normal.[21] Originally shown by von Laue (1936) and later by Andrews and Cowley[22] and Robinson,[23] the external surfaces give rise to streaks emanating from each Bragg peak of reciprocal lattice; the streaks are called crystal truncation rods and their intensity profile contains detailed structural information. The streaks are indexed as discrete rods with integer h and k multiples of reciprocal lattice vectors in-plane and a continuous variable L representing the perpendicular momentum transfer.

 ©2003 The American Physical Society

Scattered intensity from a layered structure is

$$I_{hkL}^{\mathrm{CTR}} \propto |F_{hk}^{\mathrm{bulk}}|^2 \frac{1}{4\sin^2(\pi L)}, \tag{1}$$

where F_{hk}^{bulk} represents the 2D structure factor of atoms in each layer. In a real surface, the atoms do not generally lie exactly at bulk lattice sites, because of interlayer relaxation, roughness, absorption of foreign atoms, and/or reconstructions. The intensity must be modified to include a separate, surface structure factor, which is added to the bulk with the appropriate phase.

$$I_{hkL} = |F_{hkL}|^2 = |F_{hkL}^{\mathrm{surf}} + F_{hkL}^{\mathrm{bulk}}|^2, \tag{2}$$

$$F_{hkL}^{\mathrm{surf}} = \sum_{j}^{N_S} f_j \Theta_j W_j e^{2\pi i(hx_j + ky_j + Lz_j)}, \tag{3}$$

$$F_{hkL}^{\mathrm{bulk}} = \sum_{j}^{N_B} f_j W_j e^{2\pi i(hx_j + ky_j + Lz_j)} \frac{1}{1 - e^{-2\pi i L}}, \tag{4}$$

where

$$W_j = e^{-B_j Q^2/(16\pi^2)}, \tag{5}$$

with f_j the atomic scattering factor of atoms in layer j, B_j the Debye-Waller parameter of layer j, Q the total momentum transfer, (hkL) the Miller indices and $(xyz)_j$ the position of atom j in fractional coordinates. It is of special interest to study of damage caused by ion irradiation to include surface defects in the evaluation of F_{hkL}^{surf}. The simplest defect is caused by the missing atoms which we represent through $0 < \Theta_j < 1$ which defines the occupancy, or probability of a site being occupied, of the atoms in the jth layer.

Since Si has the crystal structure of diamond, it has a nonprimitive unit cell containing two atoms (bilayer). This makes two possible "ideal" terminations (i.e., planar truncation of the bulk) of the (111) surface. These are denoted by "double layer" (D) and "single layer" (S) termination. A D surface has fewer dangling bonds than a S surface. A hexagonal co-ordinate system for Si has been chosen for both measurements and calculations. The unit cell is defined by $a = b = a_0\sqrt{\frac{3}{8}}$, $c = a_0\sqrt{3}$ and $\gamma = 120°$, where $a_0 = 5.43$ Å is the cubic lattice parameter. The bulk 1×1 unit cell model is described in Fig. 1. Each 1×1 unit cell consists of six atoms within three bilayers at three (x,y) positions $A(0,0)$, $B(2a/3,b/3)$, and $C(a/3,2b/3)$. The stacking sequence of atoms in z direction is CcBcAa for each unit cell, where upper case refers to upper half of the double layer and lower case to the lower half.

The clean Si(111) surface reconstructs to a 7×7 structure which is widely accepted to be given by the dimer-adatom-stacking fault (DAS) model.[24] The model (Fig. 2) consists of a triangular lattice of "islands," connected to the bulk by alternately "normal" and "faulted" stacking sequences, with each island containing 21 atoms per 7×7 unit cell. Between the islands in the third layer lies a network of "dimers" containing 18 atoms per 7×7 unitcell joining them together.

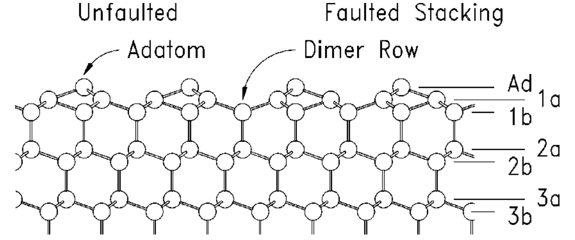

FIG. 1. Side view of the Dimer-Adatom-Stacking (DAS) fault model of the reconstructed Si(111)7×7 surface. All atoms are unrelaxed "ideal" positions as defined in DAS model. The layer notations used to mark the layer positions (z_j). Layer notations Ad, 1a, and 1b correspond to the adatom, stacking fault, and dimer atom layers, respectively. Layer notations 2a–3b correspond to the bulk layers. See the text for details.

On top of this sits an array of 12 "adatoms" per 7×7 unit cell each satisfying three bonds that would otherwise dangle from the island layer. When an ideal 7×7 reconstructed surface is folded into a 1×1 unit cell, the layer occupancies (Θ_j) for adatoms are $\frac{12}{49}$, for stacking fault $\frac{21}{49}$, and for dimers $\frac{48}{49}$. Figure 2 shows a top view of a complete 7×7 unit cell and Fig. 1 shows a side view of part of DAS model that defines the layering of the surface to bulk used for model calculations. In our calculations we have used the vertical and in-plane coordinates measured previously.[24–28] Evaluation of Eq. (2) for the published model of Si(111)7×7 gives a CTR profile shown in Fig. 3.

Partial occupancy is a very general way to model surface roughness. Over the coherence length of the x-ray beam, a surface will likely not be flat at the atomic level and will rather contain terraces, vacancies, or steps. The presence or absence of extra partial layers of atoms will cause interfer-

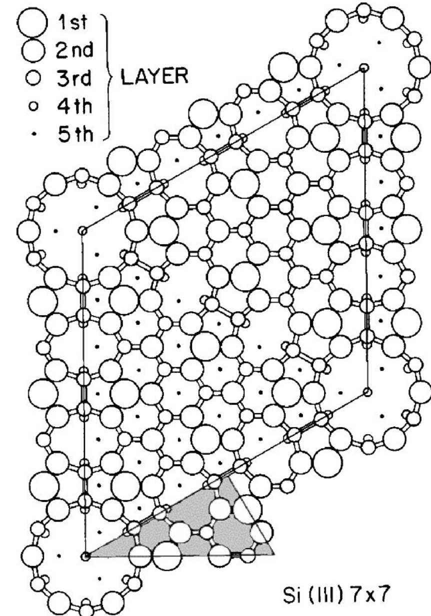

FIG. 2. Top view of full unit cell of the DAS model (Ref. 24) of Si(111)7×7 with one asymmetric unit shaded. Adatom, stacking fault and dimer layers are labeled by first, second, and third layers and bulk layers are labeled by fourth and fifth layers.

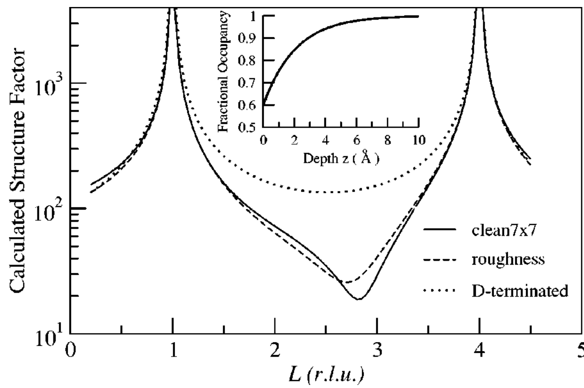

FIG. 3. Calculated structure factor of a (10L) crystal truncation rod (CTR) for the published model of Si(111)7×7 as a function of perpendicular momentum transfer L. Also shown are the CTR profile for a D-terminated bulk structure and the CTR profile for a rough Si(111)7×7 surface. Roughness is represented as fractional occupancy [Eq. (6) with $A_r = 0.4$ and $K_r = 4.5$ Å] profile with respect to depth (z) shown as an inset.

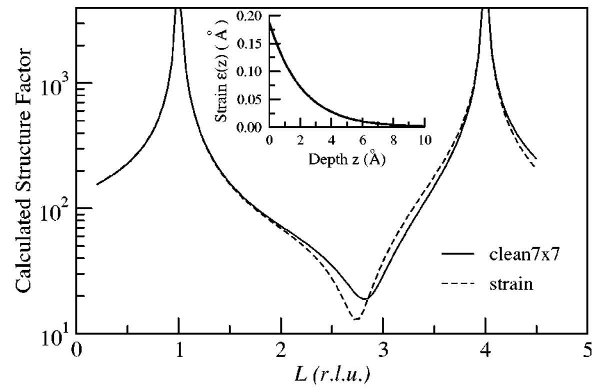

FIG. 4. Calculated structure factor of a (10L) crystal truncation rod (CTR) for the published model of Si(111)7×7 as a function of perpendicular momentum transfer L. Also shown is the CTR profile for a strained Si(111)7×7 surface. Strain profile [Eq. (7)] with respect to depth (z) shown in the inset.

ence with the diffracted wave from the bulk. This will usually cause a reduction in the intensity of the center of the truncation rod by a factor that depends on the height statistics of the surface. Various statistical models for the surface roughness and their corresponding scattered intensities have been studied and can be found in the literature.[23,29] Details about these models will be discussed later in the next sections. Here we represent roughness as the probability of the atoms in a given atomic layer to remain at lattice sites, and thus it has the same meaning as "occupancy." Since we start with relatively flat initial surfaces that are progressively eroded by sputtering, we introduce a new model of the layer probability distribution

$$\Theta_j = 1 - A_r \exp(-z_j / K_r), \tag{6}$$

where A_r and K_r are the amplitude and decay length of an exponential occupancy distribution function, respectively. As above, Θ_j is the value of the occupancy of layer j at a particular depth z_j increasing downwards from the surface at $z = 0$. A_r may include any origin offset in the definition of z.

In Fig. 3 we have shown examples of calculation for the (10L) CTR profile, corresponding to rough surface. The effect of roughness is observable between the two Bragg peaks (101) and (104). We have represented each layer by an index j, position z_j and with fractional occupancy Θ_j, as described in Eq. (6). As with all roughness models,[23,29] the function Θ_j has little effect on the CTR intensity near the Bragg peaks, where scattering is more sensitive to the bulk. It can, however, lower the intensity between the peaks, where the scattering is mostly sensitive to the surface. The inset in Fig. 3 is an example of a site occupancy distribution function as defined in Eq. (6) and the resulting effect it has on the CTR profile.

The second feature that we introduce into our (damage) model is the atomic layer displacements. It is known in general that CTR's are highly sensitive to surface relaxation, the important characteristic of whether the surface spacing is contracted or dilated. The top layer, having uncompensated bonds due to the missing layer above it, will generally not find its equilibrium configuration equivalent to bulk layers. In the case of Si(111)7×7 surface, there is a possibility of bond breaking with ion irradiation. The missing bonds will cause the top layer to move either up or down depending on the energetics of the system, a phenomenon known as relaxation. This has the effect of changing the value of the perpendicular layer spacing which shifts the intensity profile of the CTR in q space either toward larger L for contraction or smaller L for dilation.[23,30] This relaxation can in some crystals propagate many layers down and cause other layers near the top to move from their bulk positions. This relaxation of layers contributes to the lattice strain.

We introduce the following functional form for the average strain distribution within the lattice associated with the ion implantation:

$$\epsilon(z) = A_s \exp(-z/K_s), \tag{7}$$

where A_s and K_s are the amplitude and decay length of the strain distribution function, respectively. $\epsilon(z)$ is defined as the fractional layer expansion of the average crystal at depth z increasing downwards from the surface. The amplitude A_s may include any origin offset in the definition of z. The fractional strain contribution to the perpendicular layer depth z, modifies the surface structure factor. The modified position of layer j is given as

$$z_j = z_{0j} + \epsilon(z_{0j}), \tag{8}$$

where z_{0j} is the position of the unstrained layer j. The effect of a strain distribution on the scattering intensity for the CTR is shown in Fig. 4. Positive strain shifts the intensity between the Bragg peaks to smaller L.

In our example calculations, we have shown the modified CTR profile for both rough and strained layers. We have observed from the experimental CTR data for the irradiated 7×7 surfaces that the shape of the CTR profile shifts towards a bulk terminated CTR profile with dose. As the surface gets eroded the reconstructed 7×7 layers are removed, bringing the surface towards the terminated bulk structure.

The calculated CTR profile for irradiated samples are seen to change from an ideal 7×7 towards the *D*-terminated bulk profile (Fig. 3), with additional shifts observed with strain. These predictions anticipate the effects seen in our experiments.

III. EXPERIMENTAL PROCEDURE

Experiments were performed on beamline X16A of National Synchrotron Light Source (NSLS) at Brookhaven National Laboratory, which is customized for high-resolution diffraction experiments in ultrahigh vacuum (UHV).[31] The beamline uses a bent cylindrical mirror to focus bending magnet radiation into $1\,\mathrm{mm}^2$ at the sample. The incident beam is monochromatized by parallel Si(111) crystals. The diffracted beam is detected by a position sensitive detector (PSD) oriented along the surface normal behind $2\times20\mathrm{mm}^2$ slits placed 0.6 m away.

Si(111) samples were precleaned with alcohol, loaded to the UHV chamber at a pressure of about 10^{-10} Torr and degassed at about 500 °C for 6 h. Each sample was then flashed to 1200 °C and slowly cooled ($\sim$100 K/s) to 850 °C, held for 10 s annealing, and then cooled rapidly to room temperature. The surface quality was examined by monitoring the in-plane $(\frac{3}{7},0)$ and $(1,\frac{3}{7})$ reflection peaks of the 7×7 reconstruction.

The in-plane and CTR data were measured for the 7×7 clean surface before irradiation. CTR points near Bragg peaks were divided into narrow bins of PSD channels to improve L resolution. To quantitatively extract the structure factors, the intensities were integrated over orientation angle ϕ, background was subtracted and then the data were corrected for Lorentz factor and variation of active area.[18] A total of 180 scans were taken for in-plane reflections close enough to the surface plane ($L=0.2$), for perpendicular momentum transfer to be negligible. About three to four different symmetry equivalent (h,k,L) reflections for $L=0.2$, (considered to be $L=0$) were taken and averaged together assuming p6mm symmetry. Uncertainty in the measurements was deduced from the reproducibility (ϵ) which varied from 10 to 12 % on average.[18] CTR measurements were taken for the $(1,0,L)$ rod, for $0.15<L<5$ passing through Bragg peaks at $L=1$ and $L=4$. Structure factors from the symmetry equivalent $(-1,1,L)$ rod were averaged with these, assuming $p3m1$ symmetry and the reproducibility was $\epsilon=10\pm1\%$.

Ion irradiation with 200 eV Ar^+ was performed using a Varian ion gun with 5×10^{-5} Torr Ar (99.999% pure). The angle of incidence was 20°. The ion beams were rastered over the total sample area to yield uniform damage. The sample direction was fixed during the entire dosing time. Tests showed that the diffraction was unaffected by gas exposure alone. The ion current was measured at 0.1 $\mu\mathrm{A/cm}^2$ from the sample holder. The samples were dosed for four different time durations 120, 180, 300, and 600 s. The doses were estimated from time and current to be 0.75×10^{14}, 1.12×10^{14}, 1.87×10^{14}, and $3.75\times10^{14}\mathrm{ions/cm}^2$. Errors in the measurement of dose could be as high as a factor of 2, but relative measurements should be accurate to within $\sim$5%. After each dose the chamber was evacuated to UHV conditions.

TABLE I. Values of refined layer displacements from ideal DAS positions with comparison of previous works (values are in Å).

Layer name	Previous experiments			
(Fig. 1)	RHEED (Ref. 26)	LEED (Ref. 27)	X ray (Ref. 25)	(present work)
Adatom (Ad)	0.38	0.31	0.88 ± 0.2	0.4 ± 0.06
SF(1a)	-0.07	-0.12	0.08 ± 0.03	0.00
Dimer (1b)	-0.11	-0.17	0.02 ± 0.03	-0.2 ± 0.04
Bulk (2a)	-0.10	-0.08	-0.04 ± 0.03	-0.2 ± 0.04
Bulk (2b)	0.00	-0.02	-0.01 ± 0.03	0.00

IV. RESULTS

Experimental in-plane scattering data for the clean Si(111)7×7 surface were first fitted with the dimer adatom stacking (DAS) fault model given by Takayanagi[24] as a starting point for our refinement procedure of atomic position coordinates by a least squares method assuming p6mm symmetry. The least-squares fit to the clean in-plane data with refinement of 15 parameters for the displacement of positions and Debye-Waller parameters[28] gave a χ^2 value of 1.87. We have obtained the parameter values for the refined positions of the atoms, comparable fairly well with that obtained by Robinson *et al.*[28] This procedure gives the in-plane structural information for the 7×7 surface before ion irradiation.

The structure of the surface and subsurface layers can be more accurately determined using crystal truncation rod data rather than just in-plane diffraction data. Experimental CTR data for the $(1,0,L)$ rod have been fitted to a Si(111)7×7 model. Experimental CTR data from the clean Si(111)7×7 surface were fitted by refining four parameters: two vertical displacements and two Debye-Waller factors. One vertical displacement was employed for the 12 adatoms (Ad, Fig. 1) and another is for 12 dimer layer (1b, Fig. 1) atoms lying below adatoms and the layer below it (2a, Fig. 1). Two separate Debye-Waller factors were fit for 12 adatoms and 18 dimers. The in-plane displacements for the 18 dimers were kept fixed to the values obtained from in-plane fitting result. With these minimum number of parameters, the clean CTR data gave χ^2 value of 1.04 suggesting the model is adequate. For comparison, the final refined z coordinates are listed in Table I along with the coordinates obtained from earlier reported models and measurements.

Figure 5 provides a pictorial comparison between observed 2D structure factors for a clean and a dosed Si(111)7×7 surface for an asymmetric section in the (h,k) plane. Certain reflections are more sensitive to ion irradiation than others. The experimental structure factors for the in-plane (h,k) reflections $(1,\frac{3}{7})$ and $(\frac{3}{7},0)$, which have contributions largely from adatoms, are shown as a function of dose in Fig. 6. Their reduction indicates the loss of the adatom contribution from the Si(111)7×7 reconstructed sur-

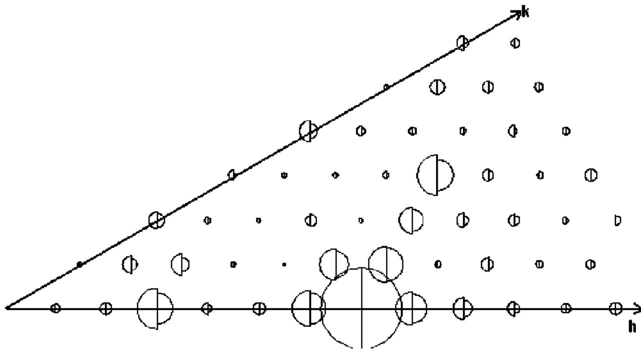

FIG. 5. (left half circles) observed structure factors for clean Si(111)7×7 surface and (right half circles) observed structure factors for ion irradiated Si(111)7×7 surface. The radius of each circle is proportional to the amplitude, the area to the intensity. Structure factors for the in-plane (h,k) reflections $(1,\frac{3}{7})$ and $(\frac{3}{7},0)$, have contributions largely from adatoms.

face. In-plane surface x-ray diffraction is one of the most appropriate technique to determine the structure of Si(111)7×7 surface and any modification therein.[30]

The in-plane diffraction data for the irradiated samples were initially fitted, using the structural fit parameters deduced from clean surface constant. Then the occupancy parameters for adatom, stacking fault, and the dimer layer atoms were varied. The parameter values obtained from the results of fitting of the in-plane data for the clean surface, and for surfaces dosed for two times (120 and 180 s), are listed in Table II. As expected, a decrease of adatom occupancies is observed. There is also a systematic reduction of stacking fault and dimer atom occupancies; these values are also listed in Table II. For the first two doses, these occupancy profiles are roughly consistent with the occupancy function as discussed in the previous section. The in-plane result shows a progressive decrease in site occupancy with depth.

CTR data from irradiated surfaces were fitted with a modified version of the clean surface model. Equation (6)

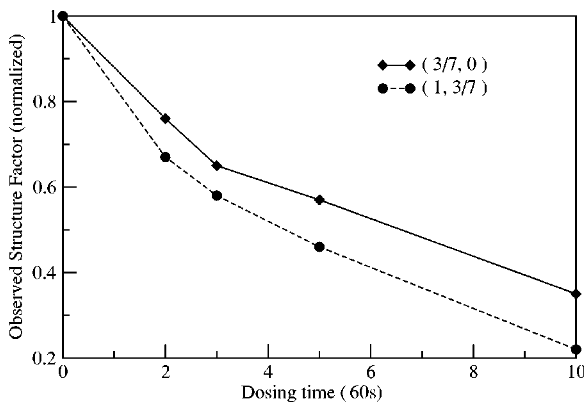

FIG. 6. Observed structure factors for Si(111)7×7 measured at $L=0.2$. Structure factors for the in-plane (h,k) reflections $(1,\frac{3}{7})$ and $(\frac{3}{7},0)$ from the irradiated surfaces (normalized to one, with the clean structure factor), falls as a function of dosing time. Error bars on structure factor values are typically about 10%.

TABLE II. Results for the occupancy of adatom, stacking fault and dimers obtained from fit to the in-plane $(L=0.2)$ data for Si(111)7×7 surface in the as prepared state and after the first two doses.

Sample		Occupancy		χ^2
(dose time)	Adatom	Stacking fault	Dimers	
Clean	1.0	1.0	1.0	1.87
120 s	0.81±.05	0.89±.05	0.91±.05	2.2
180 s	0.73±.05	0.83±.05	0.89±.05	2.5

represents the functional form of the occupancy profile. The amplitude and decay lengths define the shape and value of the function at different depth. Other forms of occupancy profiles have been tried to fit the curves. Fitting to the roughness profile (β model) as used by Robinson,[23] did not improve the fit quality for surfaces irradiated for high dose, nor did the binomial distribution of the roughness profile.[29] An error function profile was also tried for describing the occupancy profile. The fit with this profile was very close to that for the exponential function. The exponential function is preferred, however, since it requires fewer parameters and makes intuitive sense. Other functions were adequate in some cases for a single ion dose, but only the exponential function of Eq. (6) was suitable at all doses. The limited amount of information in one CTR profile means that only a few parameters can be found independently. The fits were found to be rather insensitive to the decay length, so this was constrained to a compromise value for all doses. The justification for fixing the value of the decay length is discussed below. The reduced occupancy of each layer is modeled to include the absence of atoms from that layer (missing atoms) including the static Debye-Waller factor representing the site disorder of the atoms from its position in that layer.

The initial fit to the CTR data on irradiated samples with the exponential occupancy function gave fits with a χ^2 value of 1.2. For the first two doses, the values for the adatom layer occupancy were 0.25±0.05 and 0.10±0.08, respectively. These values are in poor agreement with the in-plane results of 0.81±0.05 and 0.73±0.05, respectively. We expect that the in-plane results are more reliable than the CTR measurements for these first two doses because they include a much larger number of independent measurements. We therefore fit the CTR data with an occupancy function whereby the occupancies for the first three layers were forced to match the in-plane results. The first two doses where the in-plane results are more reliable were fitted with a known occupancy function (6), with amplitude $A_r=0.19$ and 0.21, respectively, and decay length (K_r) as 4.5 Å equal for both. Since this procedure did not yield a better fit to the data, a different physical explanation is required to allow a single model to fit both the CTR data and the occupancy function derived from in-plane results.

In Sec. II Eq. (7) was defined as the strain profile inside a crystal after ion implantation. With a known profile for the occupancy and unknown parameters for exponential strain profile, we attempted to fit the experimental CTR data for the first two doses (120 and 180 s). We indeed obtained a good

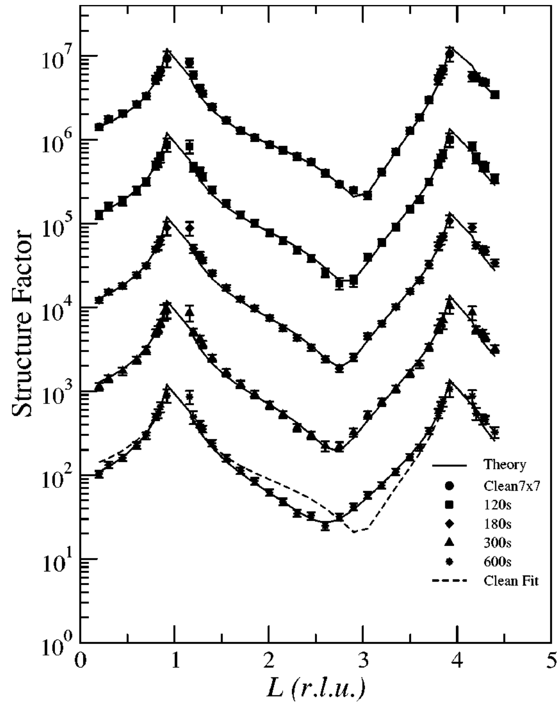

FIG. 7. Experimental $(10L)$ CTR data (symbols) and the fitted theoretical CTR curves (solid line) for clean and ion irradiated Si(111)7×7 surfaces for different doses. Curves for different doses are shifted vertically for clarity. The theoretical fit curve for clean Si(111)7×7 surface (dashed line) is overlapped on the highest dosed data to visualize the change of symmetry of the curve with dose.

fit ($\chi^2=1$ and 1.05) which was consistent with the in-plane results. The strain amplitude (ϵ^L) for the first two doses were 0.16 % and 0.19 % with equal decay lengths $K_s=\sim 4.5$ Å. There was an increase in strain amplitude with the increase in dose. Since we have no prior knowledge of the occupancy profile for the higher-dose data, we have fitted the data with positive strain amplitude, occupancy profile amplitude and decay length as free parameters. The values for the decay length for both the profiles, occupancy and strain were ~ 4.5 Å, suggesting that the range for the effect of atom removal and layer strain in Si were nearly equal. For higher doses (300 and 600 s), the strain amplitudes were 0.21 and 0.23 %, respectively, suggesting a small increase in the strain amplitude with increasing ion dose. Finally, an additional parameter, the adatom occupancy, was also considered, and varying it led to a still better fit.

The values of the final occupancy for the adatom layer for the four doses were 0.73, 0.58, 0.39, and 0.17 (Fig. 6). These values were very close to the average of experimental structure factors for $(\frac{3}{7},0)$ and $(1,\frac{3}{7})$ reflections normalized to 1(clean value) as shown in Fig. 6. With all the above discussed parameters, the experimental CTR data for all the four doses were fitted with χ^2 values between 1 and 1.2. Figure 7 shows both experimental data and the fits for the clean irradiated surfaces. Figure 8 shows the occupancy profiles with respect to the sample depth. The dotted curve in Fig. 8 illustrates that the additional adatom layer occupancy is lower than that

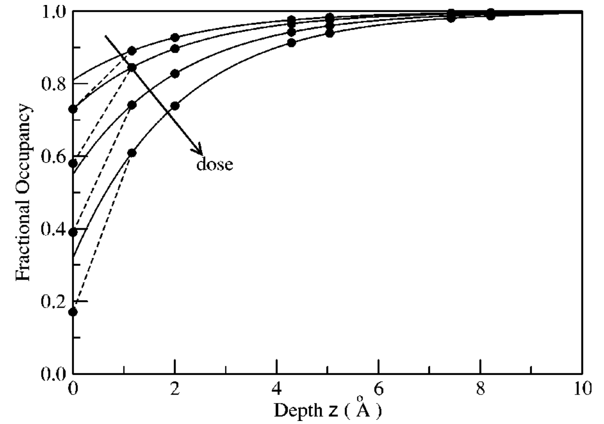

FIG. 8. (solid line) Occupancy profiles obtained from the fit parameters A_r and K_r using Eq. (6) for different ion dosing time. (Dashed curve) Extrapolated profiles for additional reduction in adatom occupancy. (Solid dots) The positions of different layers (Fig. 1) in the z direction.

suggested by a pure exponential decay. Figure 9 shows the strain profile obtained for different doses with respect to sample depth starting from the surface layer.

V. DISCUSSION

The DAS model[24] is widely accepted for the Si(111)7 ×7 reconstructed surface and forms a consistent starting point for the discussion of our results. On a Si(111)7×7 surface, bombardment with rare-gas ions has been reported to sputter surface adatoms in the low-energy range.[10–13] Our experiments found similar effects during irradiation with 200 eV Ar^+ ion on Si(111)7×7 surface at an incidence angle of 20°. Since the dimer, adatom, and stacking fault layers have unique signatures in the diffraction pattern, it is possible to measure the initial rate of erosion directly from the estimation of the missing atoms in each layer. Figure 8 shows the results for the site occupancy profile in irradiated samples. Beyond the first layer, our results are consistent with an exponential reduction of occupancy with depth. The amplitude of the exponential function increases with dose.

The decaying occupancy profile can be considered to con-

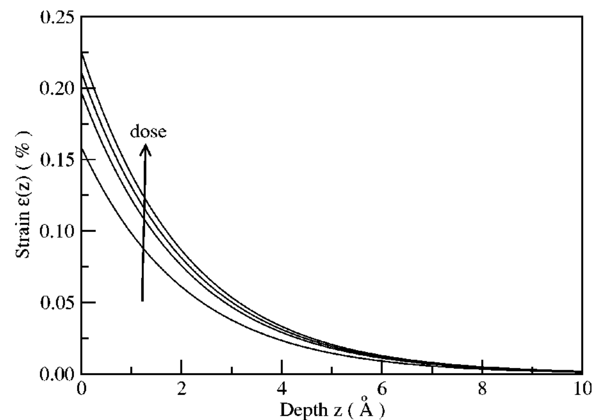

FIG. 9. Strain profiles obtained from the fit parameters (Table III) A_s and K_s using Eq. (7)for different ion dosing times.

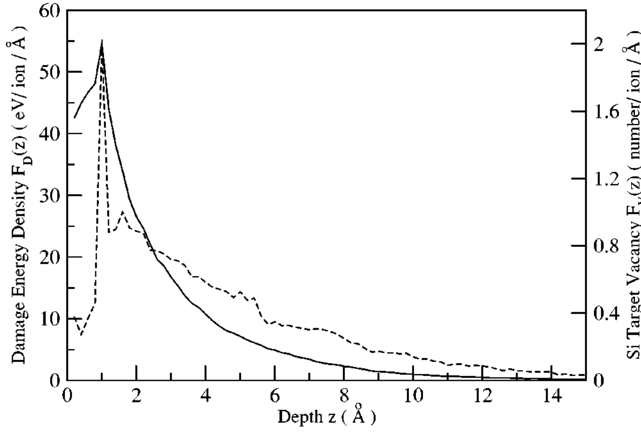

FIG. 10. Distribution profile for the damage energy density $[F_D(z)]$ (solid line) and Si target vacancy $[F_V(z)]$ (dashed line), with respect to target depth (z) for 200 eV Ar ion interaction with Si target obtained from the SRIM2000 Monte Carlo simulation. See the text for details.

sist of different depth of craters formed due to progressive ion bombardment. It is sometimes seen in STM measurements that a crater forms with different appearance, depending on the ion energy and size.[12] There is also a possibility of missing atoms in deeper layers than just the surface. Moreover the disordering of atoms from different layers contributes to the static Debye-Waller factor. The combined contribution of missing atoms and disordering of atoms at different layers is described by the occupancy profile (Fig. 8).

Results from SRIM2000 Monte Carlo simulations[17] on the damage energy distribution $[F_D(z)]$ and Si target vacancy distribution $[F_V(z)]$ of 200 eV Ar ions impinging on Si at an angle of 20° are shown in Fig. 10. A displacement energy of 15 eV and a surface bonding energy of 5 eV were employed in this simulation. Since the ion energies are low ($<$200 eV), the calculations should be considered very approximate. Incident Ar^+ ions for our conditions tend to form more surface defects than bulk defects[8] and the vacancy distribution overall shows an exponential shape. Since the number of missing atoms from different layers depends on the vacancy created in that layer, we therefore consider it reasonable to expect an exponential distribution for the occupancy profile that mimics the vacancy distribution profile. Our fitting results indeed resemble the functional dependency for the site occupancy for atoms in different layers. We observed however, a larger reduction in the occupancy for the adatoms, suggesting an unusually sensitive configuration there. This is attributed to the different bonding configuration of the adatoms on the Si(111)7×7 surface.

In further comparing our results with the vacancy distribution determined from SRIM we observe that the decay length of the occupancy profile is of $K_r = 4.5$ Å (Table III), whereas $F_V(z)$ falls to it's $1/e$ value at depth of $\sim$3.0 Å (Fig. 10). This shows reasonable agreement between the CTR fit with the SRIM results in considering the assumptions in SRIM.

It has been previously reported that implantation of keV-energy ions in Si and Ge, causes strain which scales with dose and depends on the amount of energy deposited per ion

TABLE III. Results for the occupancy profile parameters (A_r, K_r) and strain profile parameters (A_s, K_s) obtained form the fit to CTR data for Si(111)7×7 structure. Error bars for all the parameters are about 5%.

Sample (dose time)	Occupancy A_r	Parameter K_r(Å)	Strain A_s(%)	Parameter K_r(Å)	χ^2
120 s	0.19	4.5	0.16	4.5	1.08
180 s	0.27	4.5	0.19	4.5	1.12
300 s	0.45	4.5	0.21	4.5	1.10
600 s	0.68	4.5	0.23	4.5	1.20

in atomic displacements.[32–34] In case of GaAs the strain increases linearly with dose in the low-dose limit (5×10^{13} ions/cm^2), but beyond which, it behaves nonlinearly.[35] The x-ray strain perpendicular to the crystal surface ϵ^L was found in these studies to follow the relationship[32,35]

$$\epsilon^L(z) = k\phi F_D(z), \tag{9}$$

where $F_D(z)$ is the average energy per ion per unit depth deposited by nuclear collision at depth z, ϕ is the irradiation dose, and k is a constant. In our case the perpendicular strain profile follows closely the SRIM calculation (Fig. 10) for $F_D(z)$ profile for 200 eV Ar^+ in Si. The dose dependence moreover was found to be approximately linear (Table III). The validity of Eq. (9), which normally applies to the higher energy (keV) range, apparently extends down to 200 eV, at least for the ion-surface interaction on the Si(111)7×7 reconstructed surface. Qualitatively the dose and energy deposition profile follows the trend of Eq. (7). If we calculate quantitatively the constant k for Si for our case using Eq. (9) with $F_D(z) = 50$ eV/ion Å and strain for the highest dose ($\phi = 3.75\times10^{14}$ ions/cm^2) sample $\epsilon^L = 0.23\%$, we obtain $k = 0.122$ Å^3/eV, which is considerably higher than the values reported[35] for keV range energy ($k = 0.0031$ Å^3/eV). Hence explanation for positive strain observation in our case could not extrapolated from the keV range of damage calculations. Strain is not correlated with the energy deposited by electronic stopping, or with the presence of the implanted atoms [up to concentration of 9×10^{-4} at. % (Ref. 35)]. In our case, a Rutherford back scattering measurement showed no trace of implanted Ar within the surface layers. Hence the contribution of impurity Ar ions for the current dose levels has no contribution to the strain directly. For our case, the positive strain could be due to the expansion of surface layers by bond breaking and subsequent increase of average bond lengths. There is excess disordering at the surface layers. This strain profile is a kind of local energy deposition effect of the ions, with strain increasing with dose.

VI. CONCLUSIONS

Surface x-ray diffraction, particularly CTR measurements, have been used to reveal the atomic level defect formation in the surface and subsurface regions of Si(111)7×7 reconstructed surface. We observed that low energy (200 eV) Ar^+

ion bombardment on Si(111)7×7 surface at an 20° incidence angle forms missing atoms at both surface and subsurface layers along with positive strain. We have demonstrated with calculations how CTR measurements are sensitive to subsurface modifications. Here we have documented how the measurement is sensitive to lattice strain and site occupancy of atoms within a few atomic layers of the surface. We have determined occupancy profiles representing the missing atom profile with depth after irradiation. We have also observed increase in strain in the subsurface layers with increase in dose. We have found a clear agreement of the results with SRIM calculations and followed the description of ion-solid interaction mechanism for surface and subsurface defect formation. The measurements are relevant to the current interest in the interaction of energetic (~5 eV) gas species found in the lower earth orbit (LEO) with different material surfaces.

ACKNOWLEDGMENTS

We thank W. Lehnert and P. A. Bennett for their assistance during the x-ray experiments and See Wee during the RBS measurements. We also thank I. A. Vartanyants for useful discussions. This work is supported by Air Force Office of Scientific Research MURI Grant No. F49620-01-1-0336 and by the National Science Foundation Grant No. DMR-9986160. The X16A beam line is supported by the U.S. DOE under Grant No. DEFG02-91ER45439 and NSLS is supported by DOE under Grant No. DEAC02-98CH10886.

*E-mail address: sghose@mail.physics.uiuc.edu

[1] S. M. Sze, *VLSI Technology* (McGraw-Hill, New York, 1988).
[2] J. Erlebachaer, M. Aziz, E. Chason, M. Sinclair, and J. Floro, Phys. Rev. Lett. **82**, 2330 (1999).
[3] R. Gago *et al.*, Appl. Phys. Lett. **78**, 3316 (2001).
[4] F. Ludwig, Jr., C. R. Eddy, Jr., O. Mails, and R. L. Headrick, Appl. Phys. Lett. **81**, 2770 (2002).
[5] M. Robinson, *Sputtering by Particle Bombardment I*, edited by R. Behrisch (Springer, Berlin, 1981) p. 73.
[6] J. E. Greene and S. A. Barnett, J. Vac. Sci. Technol. **21**, 285 (1982); *Ion Beam Assisted Film Growth*, edited by T. Itoh (Elsevier, Amsterdam, 1989), p. 101.
[7] E. Chason, P. Bedrossian, K. Horn, J. Y. Tsao, and S. T. Picraux, Appl. Phys. Lett. **57**, 1793 (1990).
[8] J. Y. Tsao, E. Chason, K. M. Horn, D. K. Brice, and S. T. Picraux, Nucl. Instrum. Methods Phys. Res. B **39**, 72 (1989).
[9] A. Al-Bayati, K. Orrman-Rossiter, R. Badheka, and D. Armour, Surf. Sci. **237**, 213 (1990).
[10] A. Takashima, H. Hirayama, and K. Takayanagi, Phys. Rev. B **57**, 7292 (1997).
[11] P. Bedrossian and T. Klitsner, Phys. Rev. B **44**, 13 783 (1991).
[12] H. J. W. Zandevliet, H. B. Elswijk, E. J. van Leonon, and I. S. T. Tsong, Phys. Rev. B **46**, 7581 (1992).
[13] P. Bedrossian, M.-J. Caturla, and T. Diaz de la Rubia, Appl. Phys. Lett. **70**, 176 (1997).
[14] Kazuya Yoneyama and Keiichi Ogawa, Jpn. J. Appl. Phys. **35**, 3719 (1996).
[15] R. Smith, D. E. Harrison, and B. J. Garrison, Phys. Rev. B **40**, 93 (1989).
[16] R. Blumerthal, K. P. Caffey, E. Furman, B. J. Garrison, and N. Winograd, Phys. Rev. B **44**, 12830 (1991).
[17] The simulation was done using the standard program SRIM2000, *Stopping and Range of Ions in Matter*, by J. F. Ziegler and J. P. Biersack.
[18] I. K. Robinson, in *Handbook of Synchrotron Radiation*, edited by D. E. Moncton and G. S. Brown (North-Holland, Amsterdam, 1986), Vol. 3.
[19] E. Vlieg, J. Appl. Crystallogr. **33**, 402 (2000).
[20] B. E. Warren, *X-ray Diffraction* (Dover, New York, 1990).
[21] J. Als-Nielsen and D. McMorrow, *Elements of Modern X-ray Physics* (John Wiley & Sons, New York, 2000).
[22] S. R. Andrews and R.A. Cowley, J. Phys. C **18**, 6427 (1985).
[23] I.K. Robinson, Phys. Rev. B **33**, 3830 (1986).
[24] K. Takayanagi, Y. Tanishiro, S. Takahashi, and M. M. Takahashi, Surf. Sci. **164**, 367 (1985).
[25] I. K. Robinson and E. Vlieg, Surf. Sci. **261**, 123 (1992).
[26] A. Ichimiya, Surf. Sci. **192**, L893 (1987).
[27] H. Huang, S. Y. Tong, W. E. Packard, and M. B Webb, Phys. Lett. A **130**, 166 (1988).
[28] I. K. Robinson, W. K. Waskiewicz, P. H. Fuoss, and L. J. Norton, Phys. Rev. B **37**, 4325 (1988).
[29] D. A. Walko, Ph. D. dissertation, University of Illinois at Urbana-Champaign, 2000.
[30] I. K. Robinson and D. J. Tweet, Rep. Prog. Phys. **55**, 599 (1992).
[31] P. H. Fuoss and I. K. Robinson, Nucl. Instrum. Methods **222**, 171 (1984).
[32] C. J. Tsai, A. Dommann, M. A. Nicolet, and T. Vreeland, Jr., J. Appl. Phys. **69**, 2076 (1991).
[33] F. Cembali, A. M. Mazzone, and M. Servidori, Phys. Status Solidi A **91**, K125 (1985).
[34] V. S. Speriosu, B. M. Paine, M-A. Nicolet, and H. L. Glass, Appl. Phys. Lett. **40**, 604 (1982).
[35] B. M. Paine, N. N. Hurvitz, and V. S. Speriosu, J. Appl. Phys. **61**, 1335 (1987).